New insights on the influence of aluminum on the anomalous hydrogen evolution of anodized magnesium using scanning electrochemical microscopy

D. Filotás[1,2], L. Nagy[1,2], G. Nagy[1,2,*], R.M. Souto[3,4,*]

[1] *Department for General and Physical Chemistry, Faculty of Sciences, University of Pécs, Ifjúság útja 6, 7624 Pécs, Hungary.*

[2] *János Szentágothai Research Center, University of Pécs, Ifjúság u. 20, Pécs, 7624 Hungary.*

[3] *Department of Chemistry, Universidad de La Laguna, Avda. Astrofísico Francisco Sánchez s/n, E-38205 La Laguna (Tenerife), Canary Islands, Spain.*

[4] *Institute of Material Science and Nanotechnology, Universidad de La Laguna, P.O. Box 456, E-38200 La Laguna (Tenerife), Canary Islands, Spain.*

Abstract

Scanning electrochemical microscopy (SECM) in the sample generation-tip collection mode was employed to gain new insights on the effect of aluminum on the anomalous hydrogen evolution from anodically-polarized magnesium exposed to an aqueous saline solution. Various experiments were designed to investigate the processes occurring on a model Mg-Al galvanic pair in regards to the hydrogen evolution reaction occurring separately at the anodic and cathodic sites. The data obtained in this work do not support the so-called noble impurity theory for HER on anodically-polarized magnesium, whereas evidences were obtained that the dark oxy-hydroxide layer formed on this metal may exert a combined catalytic efficiency toward HER whereas imperfectly passivating the metal surface.

Keywords: corrosion; magnesium; anodic polarization; anomalous hydrogen evolution; scanning electrochemical microscopy; model Mg-Al galvanic couple.

Corresponding authors: Ricardo M. Souto, Department of Chemistry, Universidad de La Laguna, P.O. Box 456, E-38200 La Laguna, Tenerife, Canary Islands, Spain.
E-mail: rsouto@ull.es; Tel: +34 922 318067.

Géza Nagy, Department for General and Physical Chemistry, Faculty of Sciences, University of Pécs, Ifjúság útja 6, 7624 Pécs, Hungary.
E-mail: g-nagy@gamma.ttk.pte.hu.

1. Introduction

A series of advantageous properties and being the lightest metallic structural materials make magnesium and its alloys very attractive materials for a wide range of industrial and technological applications [1]. In addition, the biocompatibility of magnesium may allow its use as biodegradable bone implant [2]. However, the rapid corrosion of magnesium considerably limits its wide application [3]. Therefore, the study of the corrosion of magnesium is of great interest to elucidate its mechanism and to design methods of protection. The corrosion mechanism of magnesium remains mostly unknown due to its complexity compared to other metals, mainly due to the observation of anomalous hydrogen evolution from the corroding surface under anodic polarization conditions [4] (an effect often named as the negative difference effect, NDE [5]). This "anomalous" behavior has often been justified by postulating the formation of univalent Mg^+ ions as an intermediate of the anodic reaction [5,6], followed by the reduction of water to produce hydrogen by chemical reaction due to the high reactivity of this species [7]. However, the existence of Mg^+ in aqueous environment is not verified, and the indirect detection by Petty et al. [8] has been experimentally refuted by Frankel and coworkers [9]. Another explanation for the "anomalous" increase in current density – increased rate of H_2 evolution –invokes a catalytic character of the metal surface during dissolution [10]. Williams et al. demonstrated the existence of local cathodes on the surface of anodically polarized magnesium using the scanning vibrating electrode technique (SVET) [11], which combines with reports of higher rates of hydrogen evolution in the zones of dark corroded magnesium [12,13]. The increase in the rate of hydrogen evolution in corroded areas would support a quite simple explanation of the NDE: if anodic polarization is applied, dark layer formation is faster, hence HER becomes faster too. SVET studies seem to confirm this hypothesis. The filiform pattern of the progression of corrosion product deposition is coupled with the occurrence of anodically active zones at the front of the filiform track [14]. The net cathodic and anodic currents would increase in parallel.

Another justification for the anomalous hydrogen evolution is explored in terms of iron impurities in the magnesium matrix [15]. Williams et al. [16] invoked a galvanic coupling between magnesium and iron to account for the observation of disc-shaped corrosion spots in high concentration NaCl solution, while the filiform track appeared on the surface of the metal when the concentration of the electrolyte was decreased. In fact, the corroded surface in the dark corrosion layer could be enriched with nobler metal impurities which can act as local cathodes when in direct contact with the electrolyte [17], although it has been argued that iron enrichment on the surface of anodically polarized magnesium is a low efficiency process [18].

Interestingly, Fajardo et al. have shown that the anomalous increase of hydrogen evolution is still significant in acidic environments where the dark corrosion film is not stable and the effect of impurities was also negligible due to the ultrahigh purity magnesium used in their work [19]. This would imply that the hydrogen evolution is independent of the corrosion products, while other report suggested that a weakly passivating $Mg(HPO_4)_2$ layer decreased the rate of hydrogen evolution under anodic polarization [20]. In summary, despite the extensive literature generated on the subject, no consensus has been reached to explain the anomalous hydrogen evolution effect and we can find different and often contradictory mechanisms [3,21,22].

In recent works from our group [23,24], the currently prevailing theories on anomalous hydrogen evolution effect that invoke the catalytic properties of the $Mg(OH)_2$/MgO bilayer formed on magnesium-based materials or emphasize the role of the noble impurities on the surface were investigated using the amperometric Sample Generation – Tip Collection mode of scanning electrochemical microscopy. In those studies, the following experimental assumptions were tested on pure magnesium and on alloy AZ63 as to investigate the possible catalytic effect of the $Mg(OH)_2$/MgO bilayer, namely,

1. The rate of the hydrogen evolution reaction (HER) will be enhanced after the formation of the $Mg(OH)_2$ layer.
2. The rate of HER will be enhanced if the electrolyte contains Mg^{2+} ions so that the formation of the $Mg(OH)_2$ layer is favored.
3. Either removal or hindering formation of the $Mg(OH)_2$ layer will decrease the rate of HER.
4. Higher cathodic activity will occur from the $Mg(OH)_2$-covered surface as the potential of the metal is polarized at a more positive potential.

The experimental findings supported a catalytic effect of the $Mg(OH)_2$/MgO bilayer, whereas the comparative experiments of the pure Mg and the AZ63 alloy helped to separate the effect of the noble impurities from the catalytic effect [23,24].

The role of the alloying metal on the HER was further investigated in this work. To this end, samples containing a model Mg-Al galvanic pair were prepared, in order to study the HER separately on both metals. The galvanic connection was regarded to produce a model for the conditions developed in the microenvironment of a matrix containing nobler impurities. The actual experiments are similar to those presented in our previous works [23,24], although the SG-TC SECM maps for hydrogen reduction at the tip were recorded over the spatially-separated metals while there was galvanic connection between them. That is, the

measurements were performed under *in situ* polarization condition this time, whereas the works described in our previous reports corresponded to pre-polarized and non-polarized samples instead. In this way, we consider the results reported in this work to provide a more direct insight to the negative difference effect.

2. Experimental

The model Mg-Al galvanic system consisted of metal samples embedded in an epoxy resin sleeve (EpofixKit, Struers, Denmark). Metal strips (0.3 mm × 2 mm) of the pure metals, namely magnesium of 99.9% grade, and aluminum of 99.99% grade, were cut from plates purchased to Goodfellow (Cambridge, UK). The metal strips were allowed to protrude at the rear of the mould to produce an electrical connection between them. The samples were gradually abraded using wet abrasive paper (down to 4000 grit) and subsequently polished using alumina slurries of 1, 0.3, and 0.05 μm grain sizes. The actual electrochemical cell was fabricated by placing the sample at the bottom with the freshly polished surface facing up, and Sellotape was wrapped around the sample creating a small container for about 4 mL volume of the test electrolyte. The electrochemical cell was completed with an Ag/AgCl/(3 M) KCl electrode as reference (E^0 = +0.197 V vs. NHE) and a Pt auxiliary electrode.

Ammonium chloride, potassium chloride, sodium chloride, zinc-sulfate heptahydrate, copper-sulfate pentahydrate were purchased from Reanal (Budapest, Hungary). Magnesium-chloride hexahydrate and disodium salt of ethylenediammin-tetraacetic acid (EDTA) were supplied by Merck (Darmstadt, Germany). The solutions were filled up with ultrapure water (Millipore water system, specific conductivity $\kappa = 5.6 \times 10^{-6}$ S/cm; Merck Millipore, Billerica, MS, USA).

SECM experiments were performed using a Sensolytics instrument (Bochum, Germany) operated with an Autolab bipotentiostat (Metrohm Autolab BV, Utrecht, The Netherlands), all controlled with a personal computer. Pt microelectrodes (ME) with 25 μm diameter (Goodfellow, Cambridge, UK) were employed as tips, fabricated with a ratio between the insulating shield thickness (b) to the disc electrode radius (a), $RG = b/a$, smaller than < 10. The vertical tip-sample distance (20 μm) was established using the gentle approach procedure with the aid of an optical microscope provided with a video camera. In this way, there was no need to add any redox mediator to the test solutions, and the scans could be started right after the solution was added to the cell. Both scan lines and 2D maps were recorded at the scan rate of 25 μm s^{-1}.

3. Results and discussion

Prior to the SECM characterization, the electrical state of the model Mg-Al galvanic system was monitored by recording the potentiodynamic polarization curves of the electrically disconnected samples, and are shown in **Figure 1**. According to the mixed potential theory, the corrosion potential of electrically connected metals can be estimated from the corresponding Tafel plots of individual metals as the intersection of the anodic branch of magnesium with the cathodic branch of aluminum. The intersection point is indicated in **Figure 1** by an arrow and occurs at ca. -1.54 V vs. Ag/AgCl/(3 M) KCl. This value means that in the event of galvanic corrosion, H_2 evolution will occur on both surfaces: by cathodic reaction on Al and by NDE on Mg. Interestingly, this negative mixed potential value would also imply that the polarization procedure proposed in our previous work for the study of AZ63 [23], namely, -1.0 V vs. Ag/AgCl/(3 M) KCl, in fact corresponded to a condition in which both metals were subjected to anodic polarization. In other words, there should be no hydrogen evolution on the Al sample, whereas HER would occur exclusively on Mg if the two metals were polarized at this potential value.

To test this hypothesis, SECM scan lines were recorded over the model sample containing both metals, while a polarization of -1.0 V vs. Ag/AgCl/(3 M) KCl was applied to each metal separately, or to both metals simultaneously (i.e., the latter models the behavior of the alloy when both galvanic corrosion and anodic polarization may occur). The amperometric SECM measurements were performed using the sample generator-tip collector mode (SG-TC) by setting the potential of the Pt ME tip at -0.05 V vs. Ag/AgCl/(3 M) KCl where hydrogen oxidation takes place. **Figure 2** shows typical scan lines recorded in 1 mM NaCl solution. As expected, no evolution of hydrogen gas was observed from the Al sample under any of these conditions, while H_2 always evolved from the magnesium sample regardless of the electrical state applied to this metal. When only Mg was polarized, a level of HER similar to that recorded for the polarized galvanic couple was observed. Conversely, a milder HER could be detected on Mg due to the spontaneous corrosion of Mg when only Al was polarized. The higher H_2 evolution rates on polarized Mg are due to the negative difference effect. These observations suggest that the prepolarization experiments described in ref. [23] did not produce hydrogen from the Al-rich inclusions.

On the other hand, in the case of the galvanic connection, as indicated by the polarization plots, there must also be evolution of hydrogen on the Al sample, because E_{corr} is sufficiently negative (~ -1.54 V vs. Ag/AgCl/(3 M) KCl). SECM scan lines recorded over samples which either spontaneously corrode or are galvanically connected samples are shown

in **Figure 3**. As expected, the HER peak appeared above Al, but a significantly higher hydrogen flux was also detected above the magnesium anode. An increased rate of hydrogen evolution due to the galvanic connection could be observed. However, the HER rates cannot be compared between Al and Mg, because as we have seen previously, in the case of galvanic corrosion, HER is also very localized, so 2D maps must be recorded to get a more complete characterization of the corrosion reactions occurring on these samples. In the following experiments, amperometric SECM 2D maps related to H_2 evolution were recorded above the electrically connected Mg-Al galvanic couple, and the effect of different electrolyte compositions was studied. The electrolyte compositions considered for this study were those used previously to test the validity of the catalytic theory for the NDE in AZ63 [23] and in 99.9% purity Mg [24].

Figure 4 shows two maps depicting the hydrogen fluxes recorded on the Mg and Al samples in the model galvanic pair, obtained respectively in the absence and in the presence of Mg^{2+} ions in the test solution. The chloride concentration was the same (e.g., 2 mM) in both solutions, so the different electrochemical activities observed on the maps could only be attributed to the nature of the Na^+ and Mg^{2+} ions in the electrolyte. It can be seen that, as in our previous experiments with the AZ63 alloy [23] and 99.9% magnesium [24], the addition of $MgCl_2$ significantly enhanced the HER on magnesium (see **Figure 4B**). The distribution of hydrogen formation on the magnesium strip immersed in $MgCl_2$ solution is not uniform, but the most active areas show peaks of around 14 nA. Instead, the current barely exceeds 6 nA above the Mg strip in **Figure 4A**. The variation in the case of Al is not so striking. In both experiments, the current maxima above the Al are 8-10 nA, although the Al strip is apparently more active in **Figure 4B** since no blue-colored regions are observed on the surface. However, after repeating the measurements, this feature was not always unambiguous. This indicates that Al impurities may play a minor role in the increase in hydrogen evolution observed in our experiments containing $MgCl_2$ as the electrolyte, as it was suggested in a previous work [23].

In a subsequent series of experiments, the formation of the oxy-hydroxide layer on magnesium was prevented by adding a complexing agent for dissolved Mg^{2+} ions in the test electrolyte. EDTA was chosen for this purpose, although the composition of the reference solutions was adjusted as to compensate for the equivalent amount of EDTA with that of the Mg^{2+} ions added to the solution. Thus, in the comparative experiments described here, both solutions contained EDTA in 10 mM concentration, but in the first electrolyte, EDTA was inactivated by adding an equivalent amount of $MgCl_2$. In this way, the Mg-EDTA complex is

already formed in the test electrolyte and could not capture the Mg^{2+} formed in the corrosion reaction. The other test solution contained 10 mM EDTA + 20 mM NaCl to maintain the same total chloride ion concentration.

Figures 5A and **B** show the results of the 2D H_2 mapping experiments for the Mg-Al model pair immersed in these two electrolytes. In **Figure 5A**, the evolution of hydrogen occurs much faster on magnesium than on aluminum. This fact demonstrated that the conditions are ideal for studying the anomalous hydrogen evolution effect *in situ*. Both experiments were conducted in 10 mM EDTA, so the concern about an eventual hydrogen recombination poison role could not apply here; instead, we can see the purely complexing effect. In the case of **Figure 5B**, both metals produce lower amounts of H_2, but this time the HER is dominant over aluminum and is only slightly attenuated compared to **Figure 5A**. On the other hand, on the surface of (pure) magnesium, much less H_2 is generated. These findings demonstrate that the addition of EDTA affects HER at the magnesium surface and has no significant impact on the cathodic reaction on aluminum.

4. Conclusions

New insights on the anomalous hydrogen evolution from anodically-polarized magnesium exposed to a saline solution were gained using scanning electrochemical microscopy (SECM) with the goal to evaluate the influence of aluminum as the alloying element on this process. A model Mg-Al galvanic couple was scanned in the sample generation-tip collection mode as to understand on the potential localized effect of aluminum-rich inclusions towards the magnesium matrix in the corrosion of AZ63 magnesium alloy. The sources of hydrogen evolution from spontaneously corroding single metals and during their galvanic coupling was imaged by recording the electrooxidation current of hydrogen at a Pt microelectrode tip. In addition, similar experiments were recorded when the various material combinations were subjected to polarization at a potential value sufficient to sustain anodic reactions on both metals either separated or under galvanic coupling.

It was found that hydrogen evolution occurred on the magnesium sample always, although the rates of the HER are greatly dependent on the electrical condition of the two metals. Hydrogen evolution solely occurred over aluminum when galvanically-coupled to magnesium, because the cathodic reaction occurred on the surface aluminum during the anodic dissolution of magnesium, although even greater hydrogen evolution rates were observed above the magnesium sample in this arrangement. Conversely, no hydrogen evolution was observed above aluminum when the two metals were polarized at a potential

value that was anodic to both metals. In this way, no evidence was obtained to sustain the noble impurity theory for the anomalous hydrogen evolution effect in the corrosion of magnesium-based materials.

Acknowledgements

D. Filotás expresses his greatest gratitude to the ERASMUS+ program for the financial support of a 2-month mobility grant to the University of La Laguna. Financial support by the Spanish Ministry of Economy and Competitiveness (MINECO, Madrid) and the European Regional Development Fund, under grant CTQ2016-80522-P, The National Research, Development and Innovation Office (Budapest, Hungary) under grant K125244, and the "Environmental industry related innovative trans- and interdisciplinary research team development in the University of Pécs knowledge base under SROP-4.2.2.D-15/1/Konv-2015-0015 project is gratefully acknowledged.

References

1. T.B. Abbott, Magnesium: Industrial and research developments over the last 15 years, Corrosion 71 (2014) 120-127.
2. J. Walker, S. Shadanbaz, T.B.F. Woodfield, M.P. Staiger, Magnesium biomaterials for orthopedic application: A review from a biological perspective, Journal of Biomedical Materials Research - Part B Applied Biomaterials 102 (2014) 1316-1331.
3. S. Thomas, N.V. Medhekar, G.S. Frankel, N. Birbilis, Corrosion mechanism and hydrogen evolution on Mg, Current Opinion in Solid State & Materials Science 19 (2015) 85-94.
4. A.D. King, N. Birbilis, J.R. Scully, Accurate electrochemical measurement of magnesium corrosion rates: A combined impedance, mass-loss and hydrogen collection study, Electrochimica Acta 121 (2014) 394-406.
5. G.L. Song, A. Atrens, Recent insights into the mechanism of magnesium corrosion and research suggestions, Advanced Engineering Materials 9 (2007) 177-183.
6. Q.-H. Zhang, P. Liu, Z.-J. Zhu, X.-R. Li, J.-Q. Zhang, F.-H. Cao, Electrochemical detection of univalent Mg cation: A possible explanation for the negative difference effect during Mg anodic dissolution, Journal of Electroanalytical Chemistry, 880 (2021) 114837, 8 pp.

7. E. Ghali, W. Dietzel, K.U. Kainer, General and localized corrosion of magnesium alloys: a critical review, Journal of Materials Engineering and Performance 13 (2004) 7-23.
8. R.L. Petty, A.W. Davidson, J. Kleinberg, The anodic oxidation of magnesium metal: evidence for the existence of unipositive magnesium, Journal of The American Chemical Society 76 (1954) 363-366.
9. A. Samaniego, B.L. Hurley, G.S. Frankel, On the evidence for univalent Mg, Journal of Electroanalytical Chemistry 737 (2015) 123-128.
10. S. Fajardo, G.S. Frankel, A kinetic model explaining the enhanced rates of hydrogen evolution on anodically polarized magnesium in aqueous environments, Electrochemistry Communications 84 (2017) 36-39.
11. G. Williams, N. Birbilis, H.N. McMurray, The source of hydrogen evolved from a magnesium anode, Electrochemistry Communications 36 (2013) 1-5.
12. S.H. Salleh, S. Thomas, J.A. Yuwono, K. Venkatesan, N. Birbilis, Enhanced hydrogen evolution on $Mg(OH)_2$ covered Mg surfaces, Electrochimica Acta 161 (2015) 144-152.
13. M. Curioni, J.M. Torrescano-Alvarez, Y.F. Yang, F. Scenini, Application of side-view imaging and real-time hydrogen measurement to the investigation of magnesium corrosion, Corrosion 73 (2017) 463-470.
14. G. Williams, H.N. McMurray, Localized corrosion of magnesium in chloride-containing electrolyte studied by a scanning vibrating electrode technique, Journal of The Electrochemical Society 155 (2008) 340-349.
15. D. Höche, C. Blawert, S.V. Lamaka, N. Scharnagl, C. Mendis, M.L. Zheludkevich, The effect of iron re-deposition on the corrosion of impurity-containing magnesium, Physical Chemistry Chemical Physics 18 (2016) 1279-1291.
16. G. Williams, N. Birbilis, H. N. McMurray, Controlling factors in localized corrosion morphologies observed for magnesium immersed in chloride containing electrolyte, Faraday Discussions 180 (2015) 313-330.
17. M. Taheri, J.R. Kish, N. Birbilis, M. Danaie, E.A. McNally, J.R. McDermid, Towards a physical description for the origin of enhanced catalytic activity of corroding magnesium surfaces, Electrochimica Acta 116 (2014) 396-403.
18. D. Lysne, S. Thomas, M. F. Hurley, N. Birbilis, On the Fe enrichment during anodic polarization of magnesium and its impact on hydrogen evolution, Journal of The Electrochemical Society 162 (2015) C396-C402.
19. S. Fajardo, C.F. Glover, G. Williams, G.S. Frankel, The evolution of anodic hydrogen on high purity magnesium in acidic buffer solution, Corrosion 73 (2017) 482-493.

20. S. Lebouil, O. Gharbi, P. Volovitch, K. Ogle, Mg dissolution in phosphate and chloride electrolytes: insight into the mechanism of the negative difference effect, Corrosion 71 (2015) 234-241.
21. F. Cao, G.L. Song, A. Atrens, Corrosion and passivation of magnesium alloys, Corrosion Science 111 (2016) 835-845.
22. M. Esmaily, J.E. Svensson, S. Fajardo, N. Birbilis, G.S. Frankel, S. Virtanen, R. Arrabal, S. Thomas, L.G. Johansson, Fundamentals and advances in magnesium alloy corrosion, Progress in Materials Science 89 (2017) 92-193.
23. D. Filotás, B.M. Fernández-Pérez, L. Nagy, G. Nagy, R.M. Souto, A novel scanning electrochemical microscopy strategy for the investigation of anomalous hydrogen evolution from AZ63 magnesium alloy, Sensors and Actuators B-Chemical 308 (2020) 127691.
24. D. Filotás, B.M. Fernández-Pérez, L. Nagy, G. Nagy, R.M. Souto, Investigation of the anomalous hydrogen evolution from anodized magnesium using a novel polarization routine for scanning electrochemical microscopy, Journal of Electroanalytical Chemistry, submitted.

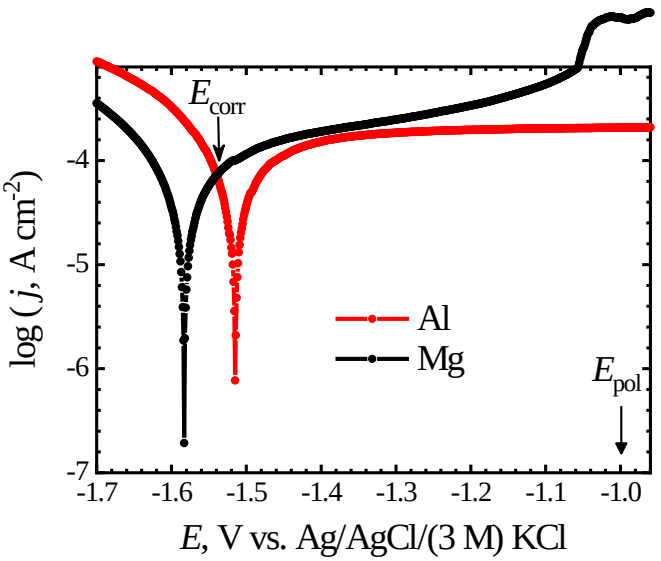

Figure 1. Potentiodynamic polarization curves recorded for pure Mg and Al strips after 30 min immersion in 1 mM NaCl. Scan rate: 5 mV s^{-1}. The reference electrode was Ag/AgCl/KCl (3M) and the counter electrode was a platinum mesh. The arrow shows the estimated potential of the galvanically connected metals. Dimensions of the metal strips: 300 μm × 2000 μm.

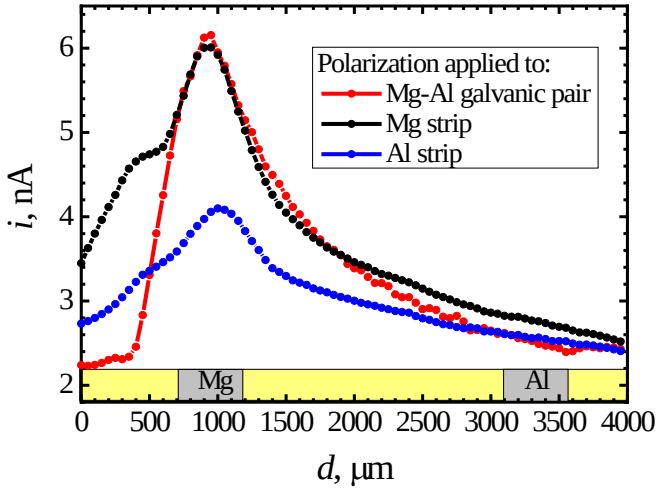

Figure 2. Amperometric SECM line scans recorded with a Pt microelectrode travelling above a model Mg-Al galvanic pair immersed in 1 mM NaCl solution. The line scans were monitored along the same pathway for an anodic polarization at -1.0 V vs. Ag/AgCl/(3 M) KCl applied to: (1) solely to one of the metals (either magnesium (black curve) or aluminum (blue curve)), and (2) simultaneously to both metals whereas they are electrically-connected at the rear of the mould (red solid line). The curves were acquired using a 25 µm diameter Pt ME with an RG < 10; E_{tip} = -0.05 V vs. Ag/AgCl/(3 M) KCl; tip-substrate distance, 20 µm; scan rate, 25 µm s^{-1}.

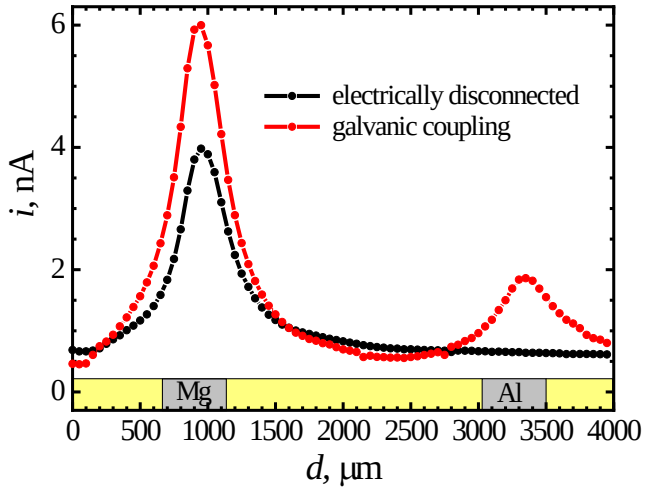

Figure 3. Amperometric SECM line scans recorded with a Pt microelectrode travelling above a model Mg-Al galvanic pair immersed in 1 mM NaCl solution. The line scans were monitored along the same pathway for the two metals: either galvanically-connected (red) or electrically-disconnected (black) during the SECM operation. The curves were acquired using a 25 µm diameter Pt ME with an RG < 10; E_{tip} = -0.05 V vs. Ag/AgCl/(3 M) KCl; tip-substrate distance, 20 µm; scan rate, 25 µm s^{-1}.

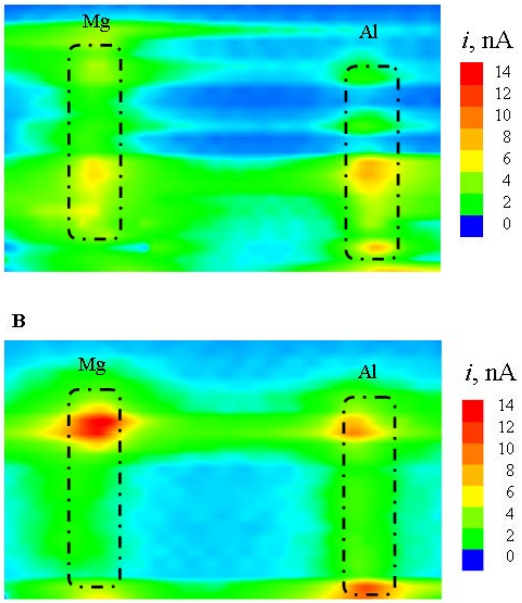

Figure 4. Amperometric SECM map scans recorded with a Pt microelectrode travelling above a model Mg-Al galvanic pair immersed in: (A) 2 mM NaCl, and (B) 1 mM $MgCl_2$ solutions. The two metals were galvanically-connected during the SECM operation. Scan dimensions: 2200 µm × 4000 µm. The curves were acquired using a 25 µm diameter Pt ME with an RG < 10; E_{tip} = -0.05 V vs. Ag/AgCl/(3 M) KCl; tip-substrate distance, 20 µm; scan rate, 25 µm s^{-1}.

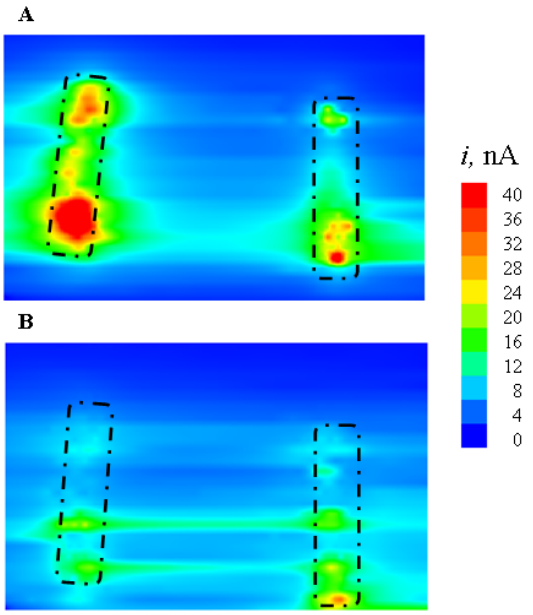

Figure 5. Amperometric SECM map scans recorded with a Pt microelectrode travelling above a model Mg-Al galvanic pair immersed in: (A) 10 mM EDTA + 10 mM $MgCl_2$, and (B) 10 mM EDTA + 20 mM NaCl solutions. The two metals were galvanically-connected during the SECM operation. Scan dimensions: 2500 µm × 4000 µm. The curves were acquired using a 25 µm diameter Pt ME with an RG < 10; E_{tip} = -0.05 V vs. Ag/AgCl/(3 M) KCl; tip-substrate distance, 20 µm; scan rate, 25 µm s^{-1}.